STEM CELLS TRANSLATIONAL MEDICINE®

TISSUE ENGINEERING AND REGENERATIVE MEDICINE

Smurf1 Silencing Using a LNA-ASOs/Lipid Nanoparticle System to Promote Bone Regeneration

PATRICIA GARCÍA-GARCÍA,[a] MARIO RUIZ,[b] RICARDO REYES,[c] ARACELI DELGADO,[a] CARMEN ÉVORA,[a] JOSÉ ANTONIO RIANCHO,[d] JOSÉ CARLOS RODRÍGUEZ-REY,[b] FLOR MARÍA PÉREZ-CAMPO[b]

[a]Department of Chemical Engineering and Pharmaceutical Technology, Institute of Biomedical Technologies (ITB), University of La Laguna, La Laguna, Spain; [b]Department of Molecular Biology, Faculty of Medicine, University of Cantabria, IDIVAL, Santander, Spain; [c]Department of Biochemistry, Microbiology, Cellular Biology and Genetics, Institute of Biomedical Technologies (ITB), University of La Laguna, La Laguna, Spain; [d]Department of Internal Medicine, Hospital U M Valdecilla, University of Cantabria, IDIVAL, Santander, Spain

Correspondence: Flor Maria Perez-Campo, Ph.D., Department of Biochemistry and Molecular Biology, Faculty of Medicine, Avda. Cardenal Herrera Oria S/N, 39011, Santander, Cantabria, Spain. e-mail: f.perezcampo@unican.es

Received May 13, 2019; accepted for publication September 17, 2019; first published October 21, 2019.

http://dx.doi.org/10.1002/sctm.19-0145

Key Words. Mesenchymal stem cells • Bone regeneration • LNA-ASO • GapmeR • *Smurf1* • Osteogenesis • BMP

ABSTRACT

Despite the great advance of bone tissue engineering in the last few years, repair of bone defects remains a major problem. Low cell engraftment and dose-dependent side effects linked to the concomitant administration of bone morphogenetic proteins (BMPs) are the main problems currently hindering the clinical use of mesenchymal stem cell (MSC)-based therapies in this field. We have managed to bypass these drawbacks by combining the silencing the *Smurf1* ubiquitin ligase in MSCs with the use of a scaffold that sustainably releases low doses of BMP-2. In this system, *Smurf1* silencing is achieved by using GapmeRs, a clinically safe method that avoids the use of viral vectors, facilitating its translation to the clinic. Here, we show that a single transient transfection with a small quantity of a *Smurf1*-specific GapmeR is able to induce a significant level of silencing of the target gene, enough to prime MSCs for osteogenic differentiation. *Smurf1* silencing highly increases MSCs responsiveness to BMP-2, allowing a dramatic reduction of the dose needed to achieve the desired therapeutic effect. The combination of these primed cells with alginate scaffolds designed to sustainably and locally release low doses of BMP-2 to the defect microenvironment is able to induce the formation of a mature bone matrix both in an osteoporotic rat calvaria system and in a mouse ectopic model. Importantly, this approach also enhances osteogenic differentiation in MSCs from osteoporotic patients, characterized by a reduced bone-forming potential, even at low BMP doses, underscoring the regenerative potential of this system. STEM CELLS TRANSLATIONAL MEDICINE *2019;8:1306–1317*

SIGNIFICANCE STATEMENT

The need to administrate high doses of bone morphogenetic proteins (BMPs) to promote osteogenesis in certain orthopedic applications, along with their associated detrimental effects, is hindering the clinical use of tissue engineering techniques in this particular field. Silencing of the *Smurf1* gene in mesenchymal stem cells (MSCs) by in situ transfecting these cells with an antisense oligonucleotide, a clinically safe approach, significantly increases the susceptibility of MSCs to BMP-2. The use of MSCs expressing low levels of *Smurf1*, together with biocompatible scaffolds that sustainably release low doses of BMP in a controlled manner, might be able to promote bone formation, avoiding the harmful effects linked to the presence of high concentration of BMPs in circulating blood.

INTRODUCTION

In recent years, there has been an increasing interest in using mesenchymal stem cell (MSC)-based approaches to improve bone repair and regeneration [1]. In particular, the use of these therapies would benefit the treatment of critical size bone defects resulting from direct trauma or from the removal of large bone areas through surgical procedures in patients with osteosarcoma, necrosis, or other pathologies. Although, for many years, autologous bone grafts have been the gold standard for the treatment of critical size bone defects, there are several drawbacks associated to these procedures, such as the limited tissue available for harvest, the extended operative time required to surgically obtain the graft, or the high percentage of morbidity at donor site. Promotion of bone repair through MSC-based therapies is a realistic approach to circumvent these limitations.

Bone tissue engineering strategies require an osteoconductive scaffold to support MSC growth and the use of osteoinducive factors,

such as bone morphogenetic proteins (BMPs), to promote MSC differentiation. Among all BMPs analyzed, recombinant human BMP-2 and BMP-7 (rhBMP-2 and rhBMP-7) have shown overall positive results on promoting bone regeneration [2]. However, BMPs are pleiotropic proteins that can exert their action on nearby tissues producing unwanted effects such as ectopic bone formation or swelling of soft tissue [3, 4]. Besides, a significant number of studies suggest the existence of undesirable dose-dependent side effects associated to the use of BMPs in the clinical practice, such as an increase in inflammatory cells at the site of application or the rise in serum levels of anti-BMP antibodies [5–11]. Moreover, BMP doses beyond a certain threshold could deregulate signaling pathways, promoting adipogenesis over osteogenesis, leading to a reduced bone quality [12, 13]. These lingering problems emphasize the importance using scaffolds that sustainably release BMPs to allow the maintenance of a minimal but adequate dose in the defect and to act as a guide to improve the new tissue formation [14, 15].

Binding of a BMP homo or heterodimer to its receptor activates downstream Smad proteins that translocate into the nucleus, where they interact with *Runx2*, the master osteogenic regulator, to activate the expression of osteogenic genes [16]. Since bone formation is a process subjected to strict regulation, once the Smad proteins have fulfilled their function, they are ubiquitinated by the HECT-type ubiquitin ligase *Smurf1* (Smad ubiquitination regulatory factor 1), and subsequently degraded by the ubiquitin-proteasome system [17]. Besides its direct implication in flagging the Smad proteins for destruction, *Smurf1* seems to have an additional function leading to the suppression of bone formation, since this protein would prevent osteoblast differentiation by decreasing the accumulation of Runx2 in these cells, and their subsequent differentiation [18].

An experimental approach that would greatly reduce the BMP dose needed to activate bone formation, thus improving the safety of the treatments, could be the abrogation of *Smurf1* expression to amplify the BMP signal. In fact, it has been recently shown that overexpression of miR-503, a microRNA targeting *Smurf1*, promotes bone formation both in vitro and in vivo in a distraction osteogenesis model [19]. In fact, our group has previously shown that knocking down *Smurf1* in rat MSCs (rMSCs) drastically increases bone formation [15]. However, although our systems proved to be highly effective in achieving bone regeneration, it harbored important disadvantages that preclude its clinical application, such as the use of viral vehicles that could integrate in the genome producing mutations, the low stability of the siRNAs used for the silencing, or the off-target effect of these molecules, able to trigger immune responses [20]. To overcome these important limitations, we have developed a new method to achieve posttranscriptional gene silencing in MSCs based on the use of locked nucleic acid antisense oligonucleotides (LNA-ASOs). These molecules can selectively and transiently regulate gene expression and their use has proven to be both clinically safe and highly effective [21, 22]. An LNA-ASO is a single-stranded deoxyribonucleotide, typically 14–20 bp long, which can specifically bind to its target mRNA directing its catalytic degradation through the action of the RNase H, an endonuclease that specifically recognizes DNA/RNA heteroduplexes and cleaves the RNA strand [23]. A particular type of ASOs, the so-called GapmeRs, has a specific design consisting of modified flanks to confer improved stability and binding, and a central DNA gap sufficient to induce RNase cleavage [24]. Currently, an important disadvantage of the treatments based on the use of ASOs is the high doses of these molecules needed to achieve the desired therapeutic effect.

To achieve transient *Smurf1* silencing through the use of low doses of GapmeRs, we have successfully used a nontoxic lipid-based delivery system [25] that highly promotes the intake of those molecules by the cells through endocytosis, making this process not only highly efficient but also economically affordable. The combination of MSCs where *Smurf1* expression has been transiently silenced and a biocompatible scaffold that sustainably release low BMP-2 doses represents a promising and safe strategy for treating critical size fractures or improving bone regeneration in patients with a decreased bone mass.

Materials and Methods

GapmeRs Design

Antisense LNA GapmeRs are 15-16-mer HPLC-purified DNA antisense oligonucleotides with full phosphorothioate (PS) substitutions (Exiqon, Qiagen, Venlo, the Netherlands). The *Smurf1* GapmeR used for silencing this gene in rats and humans is complementary to a sequence located in exon 12. As a negative control, we used Antisense LNA GapmeR Negative Control A (Ref. 300611-08). All GapmeRs were purchased as molecules labeled with fluorescein (FAM) for their subsequent detection and quantification.

MSC Isolation

Rat mesenchymal stem cells (rMSCs) were obtained from 1-month-old female Sprague–Dawley following a protocol previously described [26]. Cells were passed when they reach 80% confluence. Early passages (passage 1 or 2) were always used.

Human mesenchymal stem cells (hMSCs) were obtained from bone marrow isolated from the femoral heads of patients undergoing hip replacement surgery due to osteoporotic fractures and characterized by flow cytometry as previously described protocol [27]. All patients gave informed written consent. Study protocol was approved by the institutional review board (Comité de Etica en Investigación Clínica de Cantabria).

Cell Culture and Differentiation

All primary MSCs obtained from bone marrow, regardless of their origin (human or rat), were maintained in Mesempro RS Media (Thermo Fisher Scientific, Waltham, MA). The murine MSC line, C3H10T1/2, was cultured in Dulbecco's Modified Eagle's Medium (DMEM, Invitrogen, Carlsbad, CA, http://www.invitrogen.com) supplemented with 10% FBS and 1% penicillin/streptomycin. Cells were maintained under normoxic conditions. To promote osteogenic differentiation, cells were plated at 15×10^3 cell/cm^2 in 24 well plates and allowed to attach overnight. The following day, normal culture media was replaced with induction medium (low glucose DMEM with 10% FBS, 50 μm/ml ascorbic acid, 10 mM β-glycerophosphate, 100 nM dexamethasone) for the required time. The same

induction media was used for all primary MSCs and the C3H10T1/2 cell line.

Flow Cytometry

Cells were analyzed in a FACSCanto II flow cytometer using FACSDiva Software (BD Biosciences, San Diego, CA, http://www.bdbiosciences.com). Antibodies for human MSCs characterization have already been described [27]. The delivery efficiency of each GapmeR into cells was determined using FAM-labeled Gapmers. A minimum of 10^5 cells were harvested at indicated time points, washed in phosphate buffered solution (PBS) and resuspended in FACS Buffer (PBS, 5% Fetal Bovine Serum and 0.1% Sodium Azide) before analysis in the cytometer.

Alginate Scaffolds and Microsphere Preparation

To prepare the alginate scaffolds, 15 mg of microspheres were dispersed in 100 µl of 2% alginate (Pronova UP-MVG) in sterile MiliQ water. Then, the suspension was freeze-dried, cross-linked by incubation with a 0.15% $CaCl_2$, and after three washed with sterile MilliQ water, freeze-dried again. All the systems were stored at 4°C until use. The size and shape of the scaffolds are shown in Supplementary Figure S1. Microspheres encapsulating different amounts of rhBMP-2 (Biomedal Life Sciences, Sevilla, Spain) were fabricated by the previously described double emulsion method under aseptic conditions [15]. Briefly, 200 µl of rhBMP-2 in 0.07% polyvinyl alcohol (PVA) were mixed, using vortex (Vortex-Genie 2, Scientific Industries Inc., Bohemia, NY), with 2 ml of a PLGA (Resomer RG504, Evonik, Germany) methylene chloride solution (50 mg/ml). Then, the mix was poured into 100 ml of a 0.1% PVA (w/v) solution under constant, magnetic stirring (2 hours) for the organic solvent evaporation. Microspheres were filtered and lyophilized. Some batches were prepared with ^{125}I-BMP-2 (Perkin-Elmer) to determine rhBMP-2 encapsulation efficiency (71% $\pm$ 6%). Microspheres were visualized by scanning electron microscopy (SEM, Jeol JSM-6300) (Supplementary Fig. S1) and the microsphere volume diameter (µm) distribution, determined by laser diffractometry using a Mastersizer 2000 (Malvern Instruments) was: <76.6 (10%), <102.5 (50%), and <193.5 (90%).

In vitro release assays were carried out using ^{125}I-BMP-2 as a tracer. Briefly, each scaffold was incubated separately in a solution of PBS at 37°C under orbital shaking at 50 rpm. The amount of BMP-2 released was calculated by measuring sample radioactivity at each time point.

Cell Transfection and *Smurf1* Silencing

To enhance the cellular uptake of the GapmeRs, we used a lipid transfection agent (Dharmafect, Dharmacon, Horizon Discovery, Cambridge, U.K.) and followed the manufacture's instructions. In brief, MSCs were seeded at a concentration of 2.5×10^4 cells/cm^2 and cultured in standard conditions for 24 hours prior to transfection. Four to 5 hours before transfection, culture media is replaced by Optimem-reduced serum media (Thermo Fisher Scientific). To perform the transfection, the appropriate amount of Dharmafect per sample was always added to the required amount of DMEM without antibiotics or serum. A second mix was prepared by adding the proper amount of GapmeR (30, 60, or 120 nM as stated), to the appropriate volume of serum and antibiotics free DMEM. Both mixtures were incubated for 5 minutes at room temperature (RT). Recommended volumes of all reagents will depend on the plating format. This information can be found at the manufacture's web page. The content of the GapmeR mix was added on top of the Dharmafect mix dropwise and carefully mixed by pipetting was incubated at RT for 20 minutes before it was added to the cells dropwise.

To seed the cells in the alginate scaffolds, 10^5 cells per scaffold were resuspended in a mixture containing both the transfection agent and the correspondent amount of GapmeR in DMEM without serum or antibiotics and applied directly to the scaffold. Cells were allowed to attach to the scaffold for at least 20 minutes. Longer incubation times of up to 24 hours might be used if required. The following day, enough DMEM supplemented with 10% FBS and 1% penicillin/streptomycin was added to cover the scaffold. If the scaffold was to be maintained in culture for further analysis, media was replaced every 48 hours.

In Vivo Experiments

All surgical procedures were performed under isoflurane anesthesia in sterile conditions as previously described [28].

For the rat calvaria model, 16 female ovariectomized Sprague–Dawley rats were used. The detailed procedure for creating a calvaria defect has already been published [15]. The rats were divided in four experimental groups named: BMP; BMP Cells; BMP Cells GapmeR Ctrl (negative control GapmeR); and BMP Cells GapmeR *Smurf1* (*GapmeR* specific for *Smurf1* silencing) for histological evaluation.

For the ectopic model, alginate scaffolds were implanted subcutaneously in Sprague–Dawley females. Scaffolds were seeded with un-transduced rMSCs or rMSCs transduced with the Control (CTRL) or *Smurf1* GapmeRs following the transfection conditions and experimental procedures previously described for in situ transfection. Scaffolds with no cells were also used as control. Scaffolds were incubated with the cells in the standard growing media used for those cells a minimum of 20 minutes and a maximum of 24 hours before implantation. Different combinations of scaffolds with different BMP doses (0, 3, or 6 µg) and cells transduced with a Negative control GapmeR or a *Smurf1* GapmeR were prepared. Scaffolds seeded with untransfected cells were used as negative control. Prior to implantation in the animal, the different alginate scaffolds were transferred to a serum-free culture media and incubated at 37°C with rotation for 90 minutes and excess media was removed before implantation. All different scaffolds tested were surgically implanted in the same animal to avoid individual variations. Four animals were used for this experiment, each of them receiving eight different scaffolds. Insertion of the scaffold was performed through a cut in the skin of approximately 0.5 cm. To close the incision the skin was stapled. The same experiment was carried out in four different animals. Twelve weeks after the procedure, animals were euthanized by CO_2, implants were removed from the rats, and fixed in 10% formaldehyde, decalcified, and embedded in paraffin. Five microns sections were stained with H&E [29], Masson–Goldner trichrome [30], or Sirius red [31] following standard protocols.

For the rat calvaria model, 16 female ovariectomized Sprague–Dawley rats were used. The detailed procedure for creating a calvaria defect has already been published [15]. The

rats were divided in four experimental groups of four rats each named: BMP (scaffold with BMP-2 and no cells); BMP + Cells (scaffold with 6 μg BMP-2 and MSCs); BMP + Cells + GapmeR Ctrl (scaffold with 6 μg BMP-2 and MSCs transfected with a negative control GapmeR); and BMP + Cells + GapmeR *Smurf1* (scaffold with 6 μg BMP-2 and MSCs transfected with a GapmeR specific for *Smurf1* silencing).

All the experiments were reviewed and approved by the Animal Care Committee at the University of Cantabria and the University of La Laguna.

Histology and Histomorphometrical Evaluation of Calvarial Defect

Samples were prepared for histological analysis, as previously described [32]. New bone formation was identified by hematoxylin-erythrosin staining. The degree of new bone mineralization was assessed with VOF trichrome stain, in which red staining indicates advanced mineralization, whereas less mineralized, newly formed bone stains blue [33].

Image Analysis and Bone Quantification

Sections were analyzed by light microscopy (LEICA DM 4000B). A region of interest (ROI) for quantitative evaluation of new bone formation was defined as the area of the tissue within the defect. The ROI consisted of a circular region of 50 mm^2; the center of which coincided with that of the defect site. New bone formation was evaluated using between 8 and 10 sections of 8 μ in thickness obtained at different levels of the calvaria defect. The newly formed bone inside the defect site was identified histologically and the repaired area was measured using a detection system based on color differences with the computer-based image analysis software (Leica Q-win V3 Pro-image analysis system, Barcelona, Spain). The percentage of repair was calculated applying the equation:

$$\%\text{repair} = \frac{\text{new bone area}}{\text{original defect area within the ROI}} \times 100$$

Inmunofluorescence

For immunofluorescence assays, cells cultured into alginate scaffolds were fixed with 4% paraformaldehyde for 1 hour at RT followed by two washes with PBS1X for 5 minutes and permeabilization with 0.5% Triton X-100 in PBS for 20 minutes. For blocking unspecific binding, alginate scaffolds were incubated in 3% BSA in PBS for 20 minutes and washed twice with PBS 1X for 5 minutes. Scaffolds were incubated with the primary antibodies for 48 hours at 4°C. Primary antibodies were a rabbit monoclonal antibody against RUNX2 (DIL7F, Cell Signaling Technology, Beverly, MA, http://www.cellsignal.com) and a rabbit polyclonal against Collagen I (ab3471, Abcam, Cambridge, U.K., http://www.abcam.com). After incubation with the primary antibodies, samples were washed and incubated with an anti-rabbit IgG conjugated with FITC (Jackson InmunoResearch Laboratories, 11-095-045) for 1 hour in the dark. Nuclei were detected with DAPI-like Hoechst. Scaffolds were mounted in Prolong Gold (Invitrogen) and samples analyzed 24 hours later.

Fluorescence and Laser Scanning Microscopy

To quantify the GapmeR uptake after in situ transfection by fluorescence microscopy, we used an epifluorescence microscope (Axioplan Zeiss). Cells were staining with DAPI to visualize the nucleus. At least 200 cells were counted for each of the samples.

To quantify the percentage of fluorescent cells after the transfection with the GapmeR, a total of 100 cells was scored for each area analyzed. Total cell number corresponds to the number of nuclei (stained with DAPI); a cell was considered positive when it showed a clear green fluorescence due to the presence of the FAM-labeled GapmeR.

Confocal microscopy was performed with an LSM510 laser scanning microscope (Zeiss) and an A1R Microscope (Nikon). Confocal Scans were acquired with the LSM510 software.

Immunohystochemistry

Immunohistochemical stainings were performed as previously described [34] and anti-Col1a1 antibody (ab34710, Abcam). All staining were performed on formalin-fixed, paraffin-embedded tissue sections, which were deparaffinized and rehydrated followed by incubation with the primary antibody.

Gene Expression Analyses

RNA isolation from cell cultures and cDNA synthesis was performed as previously described [27]. *Alpl* and *Runx2* gene expression levels were measured by real-time qPCR using Taqman assays (Thermo Fisher Scientific) using assays Hs00758162_m1 and Taqman Hs00231692_m1, respectively. Expression levels were calculated relative to GAPDH (Assay reference Hs99999905_m1) or RPL13A (Assay reference Hs04194366_g1) as $2^{-\Delta ct}$.

Alkaline Phosphatase Activity Assay

MSCs were plated at 25×10^3 cells/cm^2 and cultured for 3 days in the correspondent differentiation media with or without the addition of BMP, as stated in the text. Determination of alkaline phosphatase activity in cell lysates was performed as previously described [35].

Statistical Analysis

For all experiments, except for the rat calvaria experiment, statistical significance was determined by the Student's *t* test. Data are presented as means ± standard error of the mean values. For assaying the percentage of repair in the rat calvaria model, statistical analyses were performed using SPSS 21.0 software. In this case, one-way analysis of variance (ANOVA) and a Tukey multiple comparison posttest were used to compare the overall performance of the different groups. Results are expressed as mean ± SD. Significance was set at $p < .05$.

RESULTS

Efficiency of a Lipoplex System for the Intracellular Delivery of GapmeRs

In order to set up the conditions to attain a high cellular intake of the GapmeR molecules with a minimal cellular toxicity, increasing concentrations of GapmeR (30, 60, and 120 nM) labeled with a fluorophore were mixed with a constant volume

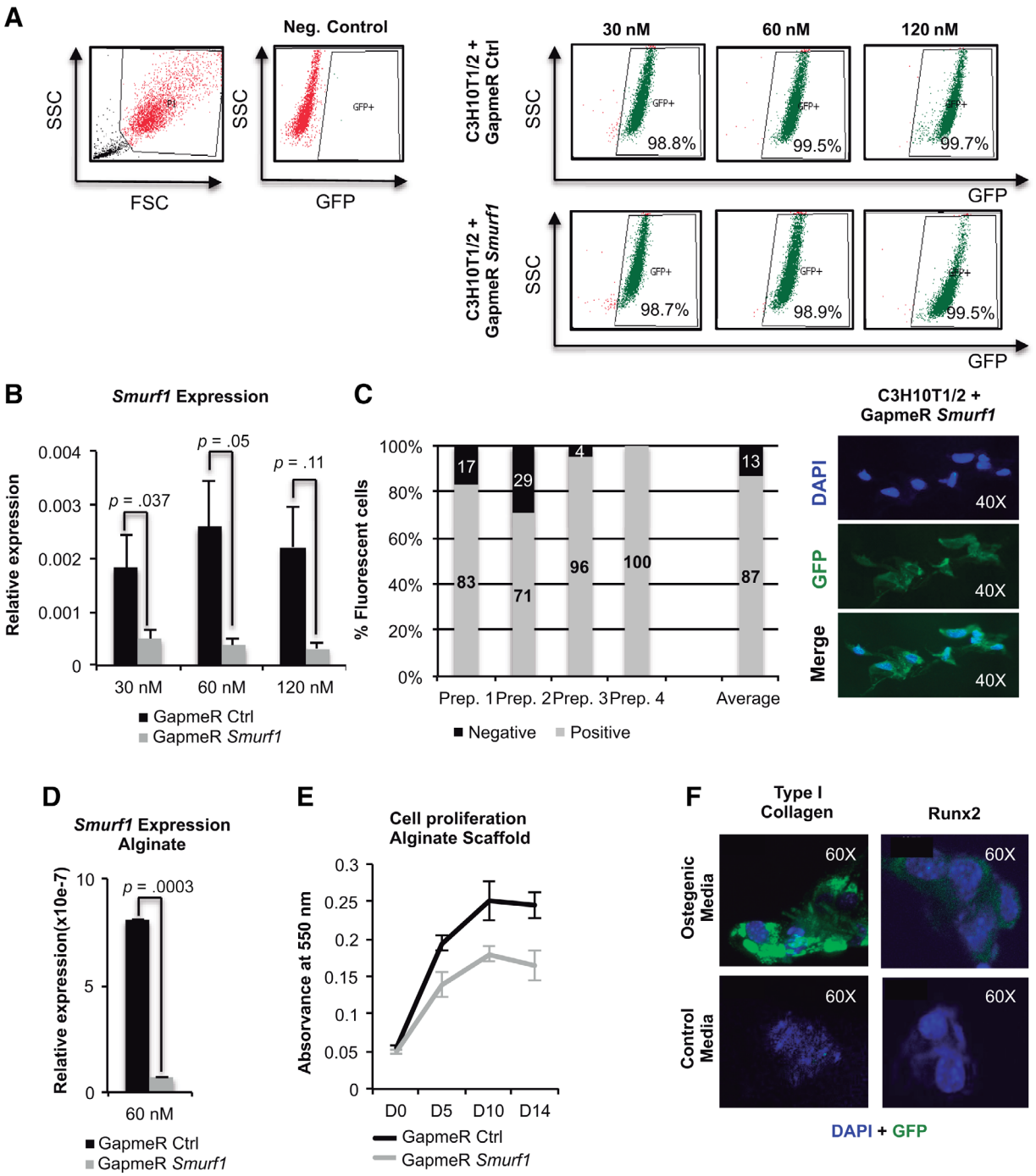

Figure 1. Setup of the locked nucleic acid antisense oligonucleotide (LNA-ASO) alginate scaffold system. **(A):** Flow cytometry profile of C3H10T1/2 mesenchymal stem cells transduced with the control and *Smurf1* LNA-ASOs. These molecules are designed to carry a fluorophore and therefore expressing GFP. Numbers show the percentage of cells positive for GFP 48 hours after transduction in each case. **(B):** PCR performed with a pair of oligonucleotides that specifically detects the Smurf1 transcript on C3H10T1/2 cells transduced with the different GapmeRs. Values reflect averages of triplicate samples. The transcript levels were normalized to GAPDH and RLP13A1 for all reactions. Bars represent standard error of the mean values. **(C):** Graph representing the percentages of fluorescent cells attached to the alginate scaffold, as showed in the picture, per 100 cells counted. The average bar represents the average values from four independent areas. **(D):** Specific PCR for the detection of the *Smurf1* transcript indicates a high degree of silencing of this gene in the cells, transfected with the *Smurf1* GapmeR, and growing onto the scaffold. **(E):** Growth curves of C3H10T1/2 cultures transduced with the different GapmeRs at different days of culture. The graph represents the absorbance of the cultures once treated with MTT. Values correspond to three independent cultures in each case. **(F):** Inmunofluorescence study of Runx2 and collagen I expression in cells undergoing differentiation in the microenvironment of the alginate scaffold. Runx2 analysis was performed at 4 days after the initiation of the induction. Col1A1 analysis was performed at day 10 of osteogenic differentiation. Cells seeded to the scaffolds growing in normal media were used as control.

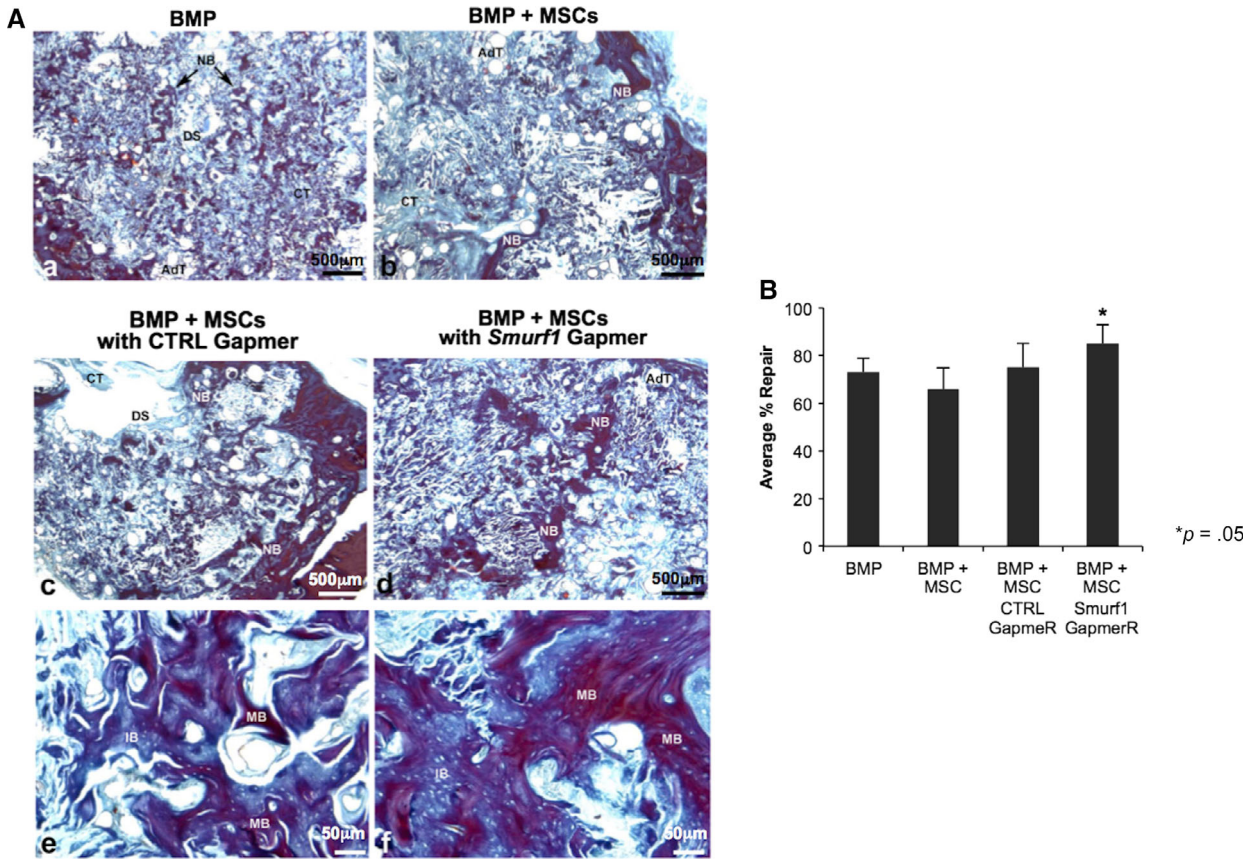

Figure 2. Bone regeneration in a calvarial critical size defect. **(A):** Sixteen female ovariectomized Sprague–Dawley were divided in four experimental groups of four rats each (n = 4). **(A–D):** Semipanoramic representative images showing in the experimental groups BMP (A), BMP Cells (B), BMP Cells LNA-ASO Ctrl, (C) and BMP Cells LNA-ASO *Smurf1* (D) the repair response where newly formed bone (NB) can be seen both on the margins and inside the defect. The images **(E)** and **(F)** show details at high magnification of the newly formed bone in the BMP Cells LNA-ASO Ctrl (E) and BMP Cells LNA-ASO Smurf1 (F) groups. Observe the greater homogeneity and continuity in the structure of the bone in the group BMP Cells LNA-ASO *Smurf1* as well as larger areas of mineralization stained red (mature bone). Abbreviations: AdT, adipose tissue; CT, connective tissue; DS, defect site; NB, newly formed bone; IB, inmature bone; MB, mature bone. (A–D) ×25, (E, F) ×200. (B) Histomorphometrical analysis. Comparison of the percentages of repair among the different experimental groups by means of a one-way ANOVA with Tukey multiple comparison posttest. Bar graph depicts percentages of repair at different experimental time points. Bars represent means ± SD, *p < .05.

of a lipidic transfection agent and used to transfect a monolayer culture of the murine MSC line C3H10T1/2. The use of this MSC line as an alternative to rat MSCs for the initial set up the transfection conditions would allow us to reduce the number of animals used in the study, therefore complying with the principles of Humane Experimentation. Flow cytometry analysis showed that GapmeRs concentrations of just 30 nM achieved more than 98% efficiency with both the control and *Smurf1* GapmeRs, compared to those treated only with the lipidic agent (Neg. Control). Higher concentrations (60 and 120 nM) did not improve transfection efficiency (Fig. 1A). Importantly, a concentration of 120 nM lead to high cell death rates 24 hours after the transfection. Analysis of *Smurf1* silencing in those samples showed an important reduction in *Smurf1* expression when GapmeR concentrations of 60 and 120 nM were used (Fig. 1B). Since the 60 nM concentration produced slightly higher levels of gene silencing and showed no substantial cell death after transfection, this concentration was chosen for the subsequent procedures.

Since we aim to use MSCs in conjunction with an alginate osteoconductive scaffold, we tested the in situ cellular uptake of the GapmeR and the ability of the transfected cells to attach and proliferate in the scaffold microenvironment. As shown in Figure 1C, 48 hours after the transfection, fluorescent microscopy analysis showed a high percentage of fluorescent cells (87% on average) attached to the scaffold, indicating that results from the in situ transfection at the scaffold are comparable to those obtained in a monolayer culture. Subsequently, cells were isolated from the alginate scaffold to assay *Smurf1* silencing. Figure 1D displays a highly significant degree of silencing when cells were transfected with the *Smurf1* Gapmer compared to those transfected with the control GapmeR. MTT analysis at different time points showed that cells transfected with both the control and *Smurf1* GapmeR were able to proliferate in the scaffold microenvironment, although small differences in the proliferation rate could be detected between the two types of cells (Fig. 1E).

We next evaluated the suitability of our scaffold to support osteogenic differentiation. To this end, we allowed untransfected cells to differentiate in an osteoinductive media for 21 days and tested the presence of osteogenic proteins (Runx2 and Collagen type I) by immunofluorescence at

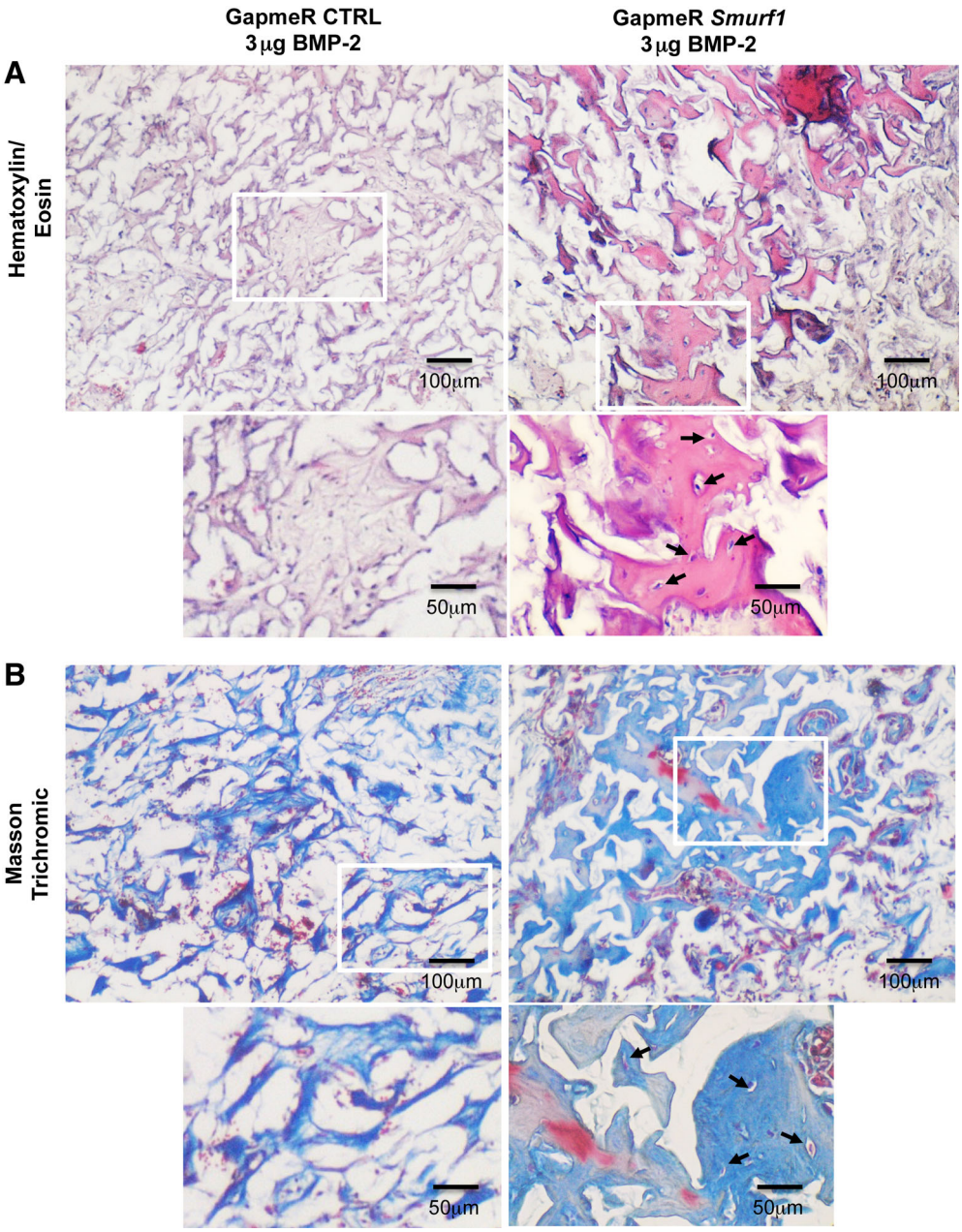

Figure 3. Hematoxylin/eosin and Masson-Goldner staining of subdermical implants in rats pictures show histological analysis of sections obtained from decalcified implants (n = 4). Hematoxylin/eosin **(A)** and Masson–Goldner staining **(B)** showing mineralized matrix in light pink and light blue respectively. Arrows indicate osteocytes-like cells surrounded by lacunae and immersed in the mineralized matrix. Magnification: ×4 and ×8.

different time points. Runx2 was detected as early as day 4 in cells undergoing osteogenic differentiation in alginate scaffolds (Fig. 1F) whereas in cells growing in a normal media, Runx2 expression was not detectable. Type I collagen was also observed in cells growing in differentiation media at a later stage (14 days) (Fig. 1F).

In Vivo Assessment of Bone Formation by *Smurf1*-Depleted rMSCs in an Osteoporotic Rat Calvaria Defect Model

To assay the in vivo bone forming capacity of *Smurf1*-depleted rMSCs, we used an alginate scaffold containing 6 μg of BMP-2 microspheres that would sustainably release BMP-2 to the site of damage in a rat calvaria defect model. BMP-2 release from microspheres in cumulative percentage was 20% ± 3.1% at 24 hours, 30% ± 1.9% at 4 days, 37% ± 4.4% at 7 days, 43% ± 6.3% at 14 days, and 55% ± 4.1% at 28 days.

The histological analysis 12 weeks postimplantation showed new bone formation in all experimental groups, including the BMP-2 only group (BMP), with an important degree of repair defect (Fig. 2A, panels a–d). The repair response was quite homogeneous in each of the implanted groups and was observed both in the margins and inside of the defect (Fig. 2A, panels a–d), with the BMP + Cells group showing the less new bone formation inside the defect (Fig. 2A, panel b). The micro-architecture of the repaired bone showed a fragmented

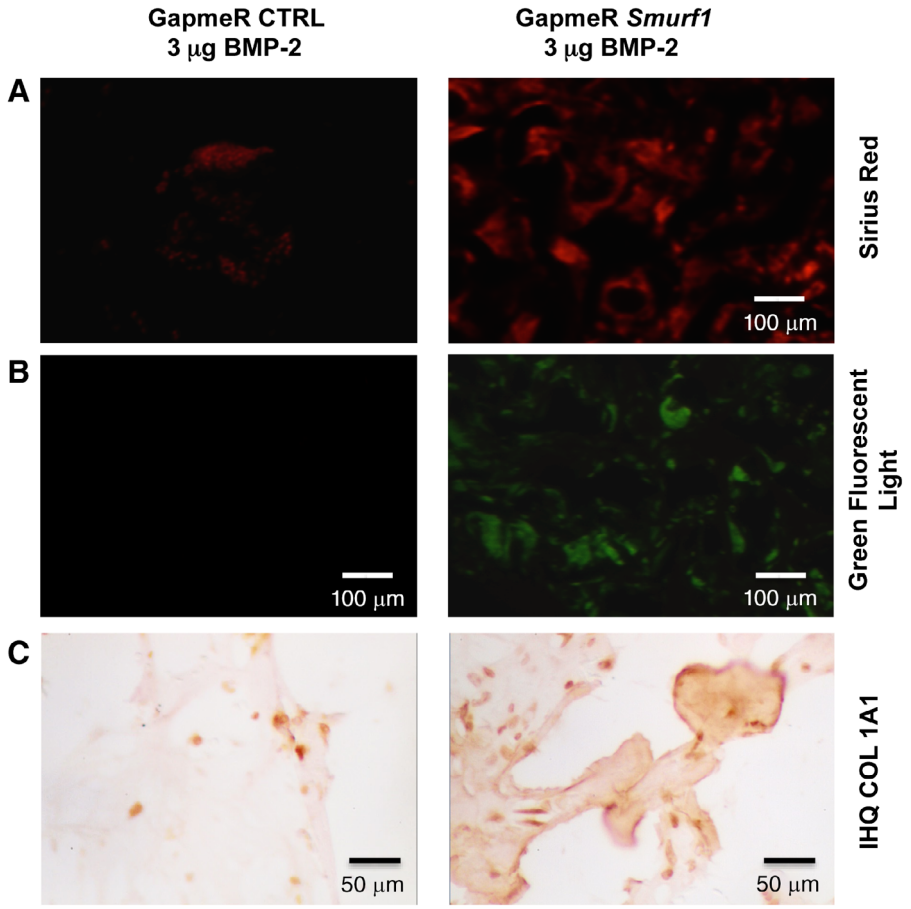

Figure 4. Sirius red-polarization/fluorescence detection of collagen fibers and immunohistochemical analysis of subdermical implants in rats. Pictures show analysis of sections obtained from decalcified implants (n = 4). **(A):** Polarization microscopy of Sirius red stained collagen fibers, showing birefringence of collagen enriched areas. **(B):** Slides observed under green fluorescent showing the typical autofluorescence of collagen fibers. **(C):** Immunohistochemistry analysis of the correspondent sections using a Col1a1 antibody where arrows indicate regions rich in COL1a1. Magnification: ×4.

appearance in most groups, with the exception of the BMP group and BMP + Cells + Gapmer *Smurf1* group, where areas of new bone were observed that showed less fragmentation and more homogeneous appearance (Fig. 2A, panels a and d). In general, there was a low presence of adipose and connective tissue, being the repaired bone structure quite similar to that of normal bone. VOF staining technique showed that most of the newly formed bone had a reddish-brown coloration (Fig. 2A, panels e and f), compatible with a good degree of mineralization (mature bone), being slightly higher in the BMP + Cells + Gapmer *Smurf1* group (Fig. 2A, panel f).

The histomorphometric analysis of the defect area showed repair percentages between 66% and 85% for the BMP + Cells and BMP + Cells + Gapmer *Smurf1* groups, respectively. The group implanted with rMSC in which *Smurf1* had been silenced (BMP + Cells + Gapmer *Smurf1*), showed a repair percent significantly higher with respect to the rest of the groups (Fig. 2B).

In Vivo Assessment of Bone Formation of *Smurf1* Depleted rMSCs in a Rat Ectopic Implantation Model

In order to exclusively analyze the contribution of transplanted rMSCs to bone regeneration in the alginate scaffold system, we used an ectopic in vivo system that would prevent rMSCs mobilized from the surround tissue seeding the scaffold. For this, we implanted the scaffolds subcutaneously in the back of Sprague–Dawley rats. We also analyzed whether the rMSC where *Smurf1* have been silenced would show a stronger response in terms of regeneration capacity that the control cells, when cells were subjected to suboptimal doses of BMP-2. To this end, rMSCs were seeded into scaffolds loaded with different amounts of BMP-2 (3 and 6 μg), and transfected in situ using the 60 nM GapmeR concentration previously chosen to achieve maximum efficiency. These scaffolds loaded with the transfected cells were then subcutaneously implanted in the recipient animals. As control, we also performed the same procedure with a mixture containing only the transfection agent and rMSCs.

After 12 weeks, the implants were surgically removed and the extent of new bone formation was analyzed by histological techniques. Scaffolds loaded with the high dose of BMP-2 microspheres (6 μg) lead to a consistent bone formation independently of whether the rMSCs had been transfected with a control GapmeR or with a GapmeR for the silencing of *Smurf1* (Supplementary Fig. S2). However, in the implants loaded with a low dose of BMP-2 (3 μM), only those rMSCs transfected with the *Smurf1* GapmeR showed abundant and mature bone matrix (Fig. 3, Hematoxilin/Eosin row). These areas of mature

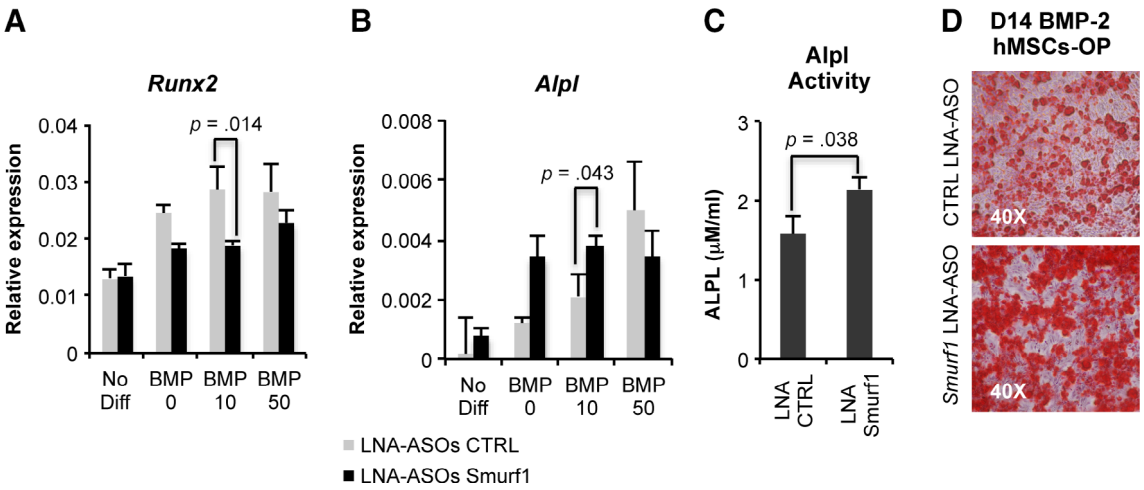

Figure 5. Differentiation capacity of hMSC from osteoporotic patients. **(A, B):** Quantitative PCRs showing the relative expression levels of different osteogenic markers (*Runx2* and *Alpl*) in hMSCs from osteoporotic patients (MSC-OP) transfected with a control GapmeR and a GapmeR for the silencing of *Smurf1*. Graphs show expression of the analyzed markers in the presence of different doses of BMP-2. Values reflect averages of triplicate samples. (B) Graph showing a significant increase in the Alpl activity in MSC-OP treated with the *Smurf1* GapmeR and differentiated for 8 days in the presence of 10 ng/ml BMP-2. **(C):** Osteogenic differentiation of the same hMSCs-OP transfected with the *Smurf1* GapmeR and differentiated in the presence of 10 ng/ml BMP-2 as revealed by Alizarin red staining bars represent standard error of the mean values. *p*-Values are indicated.

bone also contained cells surrounded by an empty region, resembling the morphology of osteocytes within osteocytic lacunae. This result was also observed when samples were stained with Masson-Goldner technique (Fig. 3, Masson Trichromic row), a widely used histological technique that stains collagen in a blue color. Importantly, in this sample, the Masson Trichromic technique showed extensive areas of red staining, corresponding to mineralized bone, where osteocytes with lacunae are also visible. This characteristic red coloration could not be seen in the 3 μM scaffolds carrying MSC transfected with the control GapmeR, but can be clearly detected in scaffolds with BMP-2 6 μM, independently of the GapmeR used to transfect the cells seeded (Supplementary Fig. S2). Staining of the samples with Sirius Red allowed us to clearly observe bright areas under polarized light, due to the refringence of collagen fibers structured in an antiparallel position, characteristic of the organized lamellar bone (Fig. 4, Sirius Red). Additionally, the typical autofluorescence of bone was also detected in these samples when observed under green fluorescent light (Fig. 4, Green Fluorescent light).

Immunohistochemistry analysis of COL1A1 expression also showed an enhanced expression of this protein in the scaffolds seeded with rMSCs where *Smurf1* has been silenced, confirming the histological results (Fig. 4, COL1A1 row).

It is important to highlight that, contrary to what we found in the calvarial model, in this ectopic model, no bone tissue formation was detected in the control scaffolds where no cells were loaded, independently of the BMP-2 dose present in the scaffold (Supplementary Fig. S3).

Smurf1 Silencing Increases the Osteogenic Potential of hMSCs from Osteoporotic Patients

To test whether the silencing of *Smurf1* has also a positive effect on the bone forming potential of MSCs from osteoporotic patients (hMSCs-OP), these cells were transfected with the *Smurf1* GapmeR and the control GapmeR using the previously established protocols. Transfected cells were grown in an osteogenic induction media containing different doses of BMP-2 (0, 10, and 50 ng/ml) to assess the expression of key osteogenic genes in those conditions. In hMSCs-OP transfected with the *Smurf1* GapmeR and differentiated in the presence of BMP-2, we detected a clear downregulation of *Runx2* expression. Interestingly, these results can be readily observed at BMP-2 concentrations 10 times inferior to those normally used to promote osteogenic differentiation of MSCs in vitro (Fig. 5A).

Analysis of *Alpl* expression in MSCs-OP where *Smurf1* has been silenced at only 10 days of differentiation showed a significant increase of *Alpl* expression at the two BMP-2 concentrations assayed (Fig. 5B). Importantly, this difference was also significant when the alkaline phosphatase activity of the same samples was evaluated (Fig. 5C). Also in agreement with an increased osteogenic capacity, Alizarin red staining showed an important presence of calcium deposits in hMSCs-OP transfected with the *Smurf1* GapmeR after 2 weeks of osteogenic differentiation compared to the same cells transfected with a control GapmeR.

Discussion

One of the main obstacles for the development of a successful MSC-based therapy is to be able to promote engraftment and osteogenic differentiation of the transplanted cells. Different MSC modifications have been designed to achieve this point [15, 36–38]. Our group has previously shown that silencing of the ubiquitin ligase *Smurf1* using a lentiviral vector carrying a specific siRNA leads to a significant improvement of bone formation [15]. Although genetic modification of MSCs by viral transfection is highly efficient, designing clinical applications based on this system is restricted due to important safety concerns [39]. We have managed to overcome this problem by transiently modifying MSCs using GapmeRs, a specific type of LNA-ASOs with enhanced stability that represent a clinically safe way to modify MSC gene expression [40, 41]. Although

GapmeRs can be taken up in the cell unassisted through a process known as gymnosis [42], this process implies the use of extremely high concentrations of the GapmeR, incurring in exceptionally high costs and, occasionally, important dose-dependent effects [43, 44]. In our system, the combination of GapmeRs with a noncytotoxic lipidic transfection agent allowed us to reduce the quantity of these molecules needed to grant the delivery to the target cell by 5,000–10,000 times, from 300 μM used on average in gymnotic processes to 30–60 nM in the lipidic agent-assisted delivery. This important reduction would dramatically increase their clinical safety at the same time that would drop the costs of the procedure, thus bypassing the main disadvantages linked the use of these molecules. Using as low as 30–60 nM of a GapmeR specifically designed to silence *Smurf1*, we have managed to obtain transfection efficiencies close to 99% without noticeable cytotoxicity, also achieving a significant silencing of the targeted gene. We have shown that a single transient transfection with the GapmeR is able to induce a significant level of silencing of the target gene, enough to prime the MSCs for osteogenic differentiation without the need of further treatments.

Although several methods combining MSCs with osteogenic factors and biocompatible scaffolds have been tested, these methods are not free of limitations. These restrictions are normally associated to the concomitant treatment with high doses of BMP-2 needed to achieve the required therapeutic effect or to the low engraftment of the transplanted MSCs. Whereas the use of low passages and specific culture conditions has increased the success of MSCs engraftment, there is currently an unmet medical need to develop strategies to promote in vitro differentiation of transplanted MSCs avoiding the adverse effects caused by the use of high doses of BMP, which would include an increase in inflammatory cells at the site of application, the rise in serum levels of anti-BMP antibodies, generalized oedema, and the appearance of heterotrophic ossifications [13].

The use of scaffolds that sustainably and locally release BMP-2 has already been shown to efficiently induce bone formation [45–47]. Using these scaffolds in a rat calvaria model, we detected a significant increase of bone regeneration when the scaffolds were loaded with MSCs transfected with the *Smurf1* GapmeR, compared to the different control samples. However, bone formation, although to a lesser extent, was also detected when we used a BMP-2 scaffold with no cells, the same scaffold harboring untransfected MSCs or MSCs transfected with a control GapmeR. These results are not completely unexpected, since the alginate scaffold is a suitable backbone for infiltrating MSCs mobilized from the surrounding skull tissue [48–50]. Our results would suggest that the implanted MSCs could be stimulated by the sustained release of BMP-2. Also, the amount of BMP-2 loaded into the scaffolds in this assay (6 g) is able to elicit bone regeneration on its own, masking the possible effect of *Smurf1* silencing in this system.

Unlike the calvaria system, the ectopic implantation model offers the opportunity to assess exclusively the engraftment of transplanted cells and the osteogenic effect of *Smurf1* silencing. The subcutaneous localization of the scaffolds would preclude the engraftment of endogenous MSCs coming from the bone marrow, although it could not be discarded that a low number of circulating MSCs could mobilize and reach the scaffold through blood vessels [51]. Based on the results from the calvaria experiment and in order to test whether *Smurf1* silencing increases the response to BMP-2, scaffolds with two different doses of BMP-2 (3 and 6 μg) were implanted at the back of the animals. Analysis of these scaffolds showed that, opposite to the calvaria model, no bone tissue has been produced in BMP-2 loaded scaffolds with any transplanted cells, underscoring the use of this subcutaneous model for the assessment of transplanted MSCs engraftment and differentiation. Although all types of MSCs tested were able to form bone tissue when seeded in scaffolds with 6 μg of BMP (Supplementary Fig. S1), scaffolds with half the dose of BMP (3 μg) were able to elicit the formation of a mature and mineralized bone matrix only when they were seeded with MSCs where *Smurf1* expression has been previously silenced. This result clearly indicates that *Smurf1* silencing is able to increase the susceptibility of MSCs to BMP-2, allowing a significant reduction of the dose of this cytokine needed to achieve a therapeutic effect.

Directing cell fate after transplantation is specially challenging in aged and osteoporotic patients. Not only the osteogenic potential of MSC from those patients is importantly reduced [52–55], but there are also several evidences pointing to an inverse correlation between donor age and proliferative capacity [56], and between donor age and responsiveness to BMP [57], something particularly important in osteoporotic individuals, since this disease is more prevalent in aged population. It is important to note that both the animals used in the calvaria experiment and the cells implanted in those animals were osteoporotic. These results underscore the regenerative potential of hMSCs where *Smurf1* expression has been silenced and encouraged us to test this potential in MSCs from osteoporotic patients (hMSC-OP). We found that hMSC-OP where *Smurf1* expression has been silenced showed a significant increase both in *Alpl* expression and Alpl activity, indicating an enhanced osteogenic activity in those cells compared to the controls. This was corroborated by the increased deposition of calcium in culture under osteogenic conditions showed by the Alizarin red staining. Previously we have shown that *Runx2* expression levels are increased in hMSCs from osteoporotic patients [27]. Although *Runx2* is an activator of important osteogenic genes, its transcription levels need to be turned down to allow terminal differentiation of osteoblast [58]. This lack of *Runx2* downregulation after the differentiation cascade has been initiated and might actually preclude osteoblasts differentiation in osteoporotic hMSCs [58]. In the present work, we show that silencing of *Smurf1* in hMSC-OP leads to a significant downregulation of *Runx2*. This would be in agreement with our previous observations and the recently described role of *Smurf1* [18] in preventing Runx2 accumulation in osteoblast. Interestingly, MSCs-OP where *Smurf1* has been silenced were able to undergo osteogenic differentiation in response to only 10 ng/ml of BMP-2, a dose 10 times lower than those normally used in other in vitro protocols (100 ng/ml) [52, 59]. INFUSE/InductOS (Medtronic/Wyet), an FDA-approved treatment that has become very prominent in the clinic, uses an absorbable collagen sponge to administer, directly to the site of damage, a dose of BMP-2 in the milligram range [60]. Taking into account the volume of our scaffold and the BMP-2 doses used in the in vivo models presented here, BMP-2 concentration in the alginate scaffold were 60 and 120 μg/ml for

the scaffolds loaded with 3 and 6 μg, respectively. These doses are clearly inferior to those administered through the INFUSE/InductOS system (1,500 μg/ml according to the product specifications). In addition, the silencing of *Smurf1* expression has allowed us to promote osteogenic differentiation of human MSCs using BMP doses in the nanogram range, which implies a 1 million times reduction of the dose used in clinic. Therefore, our approach, based on the silencing of *Smurf1* expression in hMSCs previously isolated from the patient, would allow the enhancement of osteogenic differentiation in those cells at low BMP doses.

Conclusion

The BMP-Smad signaling cascade is an effective therapeutic target to promote bone formation. Other authors have previously tried to modulate this route by using systems that, although highly effective, are not suitable for clinical use [61, 62]. Here, we have used an efficient and clinically safe approach to enhance MSC response to BMP-2 and their therapeutic efficacy. The delivery of low doses of BMP-2 in a sustained manner would avoid the alleged side effects linked to the usage of BMPs. We have demonstrated that a single transient transfection of a GapmeR specifically designed to silence the expression of the *Smurf1* ubiquitin ligase enhances osteogenesis and mature bone formation in vivo. We propose that the combined use of biocompatible scaffolds that sustainably deliver low doses of BMP-2 and *Smurf1* silencing using a LNA-ASOs in the transplanted cells would be a promising strategy for healing large areas of bone defect, contributing to improvement of bone quality and preventing fractures.

Acknowledgments

This research was supported by a grant from the Spanish Ministerio de Economia y competitividad (Project RTI2018-097324), a grant from the Instituto de Investigación Marqués de Valdecilla (IDIVAL, INNVAL 17/15), and Palex Medical S.A.

Author Contributions

P.G.-G.: collection and assembly of data; M.R.: collection and assembly of data; R.R.: collection and assembly of data, data analysis and interpretation, final approval of manuscript; A.D.: collection and assembly of data, data analysis and interpretation; C.E.: conception and design, data analysis and interpretation, final approval of manuscript, financial support; J.A.R.: provision of study material, final approval of manuscript; J.C.R.-R.: conception and design, data analysis and interpretation, final approval of manuscript, financial support; F.M.P.-C.: collection and assembly of data, conception and design, data analysis and interpretation, manuscript writing, final approval of manuscript.

Disclosure of Potential Conflicts of Interest

The authors indicated no potential conflicts of interest.

Data Availability Statement

The data that support the findings of this study are available from the corresponding author upon request.

References

1 Zigdon-Giladi H, Rudich U, Michaeli Geller G et al. Recent advances in bone regeneration using adult stem cells. World J Stem Cells 2015;7:630–640.

2 Scarfi S. Use of bone morphogenetic proteins in mesenchymal stem cell stimulation of cartilage and bone repair. World J Stem Cells 2016;8:12.

3 Chen NF, Smith ZA, Stiner E et al. Symptomatic ectopic bone formation after off-label use of recombinant human bone morphogenetic protein-2 in transforaminal lumbar interbody fusion. J Neurosurg Spine 2010;12:40–46.

4 Kawai M, Bessho K, Kaihara S et al. Ectopic bone formation by human bone morphogenetic protein-2 gene transfer to skeletal muscle using transcutaneous electroporation. Hum Gene Ther 2003;14:1547–1556.

5 Benglis D, Wang MY, Levi AD. A comprehensive review of the safety profile of bone morphogenetic protein in spine surgery. Neurosurgery 2008;62:ONS423–ONS431.

6 Carragee EJ, Hurwitz EL, Weiner BK. A critical review of recombinant human bone morphogenetic protein-2 trials in spinal surgery: Emerging safety concerns and lessons learned. Spine J 2011;11:471–491.

7 Dmitriev AE, Lehman RA Jr, Symes AJ. Bone morphogenetic protein-2 and spinal arthrodesis: The basic science perspective on protein interaction with the nervous system. Spine J 2011;11:500–505.

8 Even J, Eskander M, Kang J. Bone morphogenetic protein in spine surgery: Current and future uses. J Am Acad Orthop Surg 2012;20:547–552.

9 Hsu WK, Wang JC. The use of bone morphogenetic protein in spine fusion. Spine J 2008;8:419–425.

10 Singh K, Dumonski M, Stanley T et al. Repeat use of human recombinant bone morphogenetic protein-2 for second level lumbar arthrodesis. Spine 2011;36:192–196.

11 Jeon O, Song SJ, Kang SW et al. Enhancement of ectopic bone formation by bone morphogenetic protein-2 released from a heparin-conjugated poly(L-lactic-co-glycolic acid) scaffold. Biomaterials 2007;28:2763–2771.

12 Krause U, Harris S, Green A et al. Pharmaceutical modulation of canonical Wnt signaling in multipotent stromal cells for improved osteoinductive therapy. Proc Natl Acad Sci USA 2010;107:4147–4152.

13 James AW, LaChaud G, Shen J et al. A review of the clinical side effects of bone morphogenetic protein-2. Tissue Eng Part B Rev 2016;22:284–297.

14 Del Rosario C, Rodriguez-Evora M, Reyes R et al. BMP-2, PDGF-BB, and bone marrow mesenchymal cells in a macroporous beta-TCP scaffold for critical-size bone defect repair in rats. Biomed Mater 2015;10:045008.

15 Rodriguez-Evora M, Garcia-Pizarro E, del Rosario C et al. Smurf1 knocked-down, mesenchymal stem cells and BMP-2 in an electrospun system for bone regeneration. Biomacromolecules 2014;15:1311–1322.

16 Chen G, Deng C, Li YP. TGF-beta and BMP signaling in osteoblast differentiation and bone formation. Int J Biol Sci 2012;8:272–288.

17 Zhu H, Kavsak P, Abdollah S et al. A SMAD ubiquitin ligase targets the BMP pathway and affects embryonic pattern formation. Nature 1999;400:687–693.

18 Shimazu J, Wei J, Karsenty G. *Smurf1* inhibits osteoblast differentiation, bone formation, and glucose homeostasis through serine 148. Cell Rep 2016;15:27–35.

19 Sun Y, Xu J, Xu L et al. MiR-503 promotes bone formation in distraction osteogenesis through suppressing *Smurf1* expression. Sci Rep 2017;7:409.

20 Jackson AL, Linsley PS. Recognizing and avoiding siRNA off-target effects for target identification and therapeutic application. Nat Rev Drug Discov 2010;9:57–67.

21 Crooke ST, Witztum JL, Bennett CF et al. RNA-targeted therapeutics. Cell Metab 2018;27:714–739.

22 Stein CA, Castanotto D. FDA-approved oligonucleotide therapies in 2017. Mol Ther 2017;25:1069–1075.

23 Stein H, Hausen P. Enzyme from calf thymus degrading the RNA moiety of DNA-RNA

Hybrids: Effect on DNA-dependent RNA polymerase. Science 1969;166:393–395.

24 Fluiter K, Mook OR, Vreijling J et al. Filling the gap in LNA antisense oligo gapmers: The effects of unlocked nucleic acid (UNA) and 4′-C-hydroxymethyl-DNA modifications on RNase H recruitment and efficacy of an LNA gapmer. Mol Biosyst 2009;5:838–843.

25 Schroeder A, Levins CG, Cortez C et al. Lipid-based nanotherapeutics for siRNA delivery. J Intern Med 2010;267:9–21.

26 Fafian-Labora J, Fernandez-Pernas P, Fuentes I et al. Influence of age on rat bone-marrow mesenchymal stem cells potential. Sci Rep 2015;5:16765.

27 Del Real A, Perez-Campo FM, Fernandez AF et al. Differential analysis of genome-wide methylation and gene expression in mesenchymal stem cells of patients with fractures and osteoarthritis. Epigenetics 2017;12:113–122.

28 Rodriguez-Evora M, Delgado A, Reyes R et al. Osteogenic effect of local, long versus short term BMP-2 delivery from a novel SPU-PLGA-betaTCP concentric system in a critical size defect in rats. Eur J Pharm Sci 2013;49:873–884.

29 Cowan CM, Shi YY, Aalami OO et al. Adipose-derived adult stromal cells heal critical-size mouse calvarial defects. Nat Biotechnol 2004;22:560–567.

30 Rentsch C, Schneiders W, Manthey S et al. Comprehensive histological evaluation of bone implants. Biomatter 2014;4:e27993.

31 Tullberg-Reinert H, Jundt G. In situ measurement of collagen synthesis by human bone cells with a sirius red-based colorimetric microassay: Effects of transforming growth factor beta2 and ascorbic acid 2-phosphate. Histochem Cell Biol 1999;112:271–276.

32 Hernandez A, Sanchez E, Soriano I et al. Material-related effects of BMP-2 delivery systems on bone regeneration. Acta Biomater 2012;8:781–791.

33 Martinez-Sanz E, Ossipov DA, Hilborn J et al. Bone reservoir: Injectable hyaluronic acid hydrogel for minimal invasive bone augmentation. J Control Release 2011;152:232–240.

34 Perez-Campo FM, May T, Zauers J et al. Generation and characterization of two immortalized human osteoblastic cell lines useful for epigenetic studies. J Bone Miner Metab 2016;35:150–160.

35 Delgado-Calle J, Sanudo C, Sanchez-Verde L et al. Epigenetic regulation of alkaline phosphatase in human cells of the osteoblastic lineage. Bone 2011;49:830–838.

36 He X, Dziak R, Yuan X et al. BMP2 genetically engineered MSCs and EPCs promote vascularized bone regeneration in rat critical-sized calvarial bone defects. PloS one 2013;8:e60473.

37 Fierro FA, Kalomoiris S, Sondergaard CS et al. Effects on proliferation and differentiation of multipotent bone marrow stromal cells engineered to express growth factors for combined cell and gene therapy. Stem Cells 2011;29:1727–1737.

38 Kim D, Cho SW, Her SJ et al. Retrovirus-mediated gene transfer of receptor activator of nuclear factor-kappaB-Fc prevents bone loss in ovariectomized mice. Stem Cells 2006;24:1798–1805.

39 Hamann A, Nguyen A, Pannier AK. Nucleic acid delivery to mesenchymal stem cells: A review of nonviral methods and applications. J Biol Eng 2019;13:7.

40 Bennett CF, Swayze EE. RNA targeting therapeutics: Molecular mechanisms of antisense oligonucleotides as a therapeutic platform. Annu Rev Pharmacol Toxicol 2010;50:259–293.

41 Levin AA. Treating disease at the RNA level with oligonucleotides. N Engl J Med 2019;380:57–70.

42 Stein CA, Hansen JB, Lai J et al. Efficient gene silencing by delivery of locked nucleic acid antisense oligonucleotides, unassisted by transfection reagents. Nucleic Acids Res 2010;38:e3.

43 Kakiuchi-Kiyota S, Koza-Taylor PH, Mantena SR et al. Comparison of hepatic transcription profiles of locked ribonucleic acid antisense oligonucleotides: Evidence of distinct pathways contributing to non-target mediated toxicity in mice. Toxicol Sci 2014;138:234–248.

44 Woolf TM, Melton DA, Jennings CG. Specificity of antisense oligonucleotides in vivo. Proc Natl Acad Sci USA 1992;89:7305–7309.

45 Dang PN, Herberg S, Varghai D et al. Endochondral ossification in critical-sized bone defects via readily implantable scaffold-free stem cell constructs. Stem Cells Translational Medicine 2017;6:1644–1659.

46 Reyes R, Rodriguez JA, Orbe J et al. Combined sustained release of BMP2 and MMP10 accelerates bone formation and mineralization of calvaria critical size defect in mice. Drug Deliv 2018;25:750–756.

47 Honda Y, Ding X, Mussano F et al. Guiding the osteogenic fate of mouse and human mesenchymal stem cells through feedback system control. Sci Rep 2013;3:3420.

48 Liu L, Hu K, Wang B et al. Mobilization of endogenous stem cells: A new strategy for bone healing. Bone 2012;51:633–634. author reply 635.

49 Peng H, Usas A, Olshanski A et al. VEGF improves, whereas sFlt1 inhibits, BMP2-induced bone formation and bone healing through modulation of angiogenesis. J Bone Miner Res 2005;20:2017–2027.

50 Granero-Molto F, Weis JA, Miga MI et al. Regenerative effects of transplanted mesenchymal stem cells in fracture healing. Stem Cells 2009;27:1887–1898.

51 Kean TJ, Lin P, Caplan AI et al. MSCs: Delivery routes and engraftment, cell-targeting strategies, and immune modulation. Stem Cells Int 2013;2013:732742.

52 Heggebo J, Haasters F, Polzer H et al. Aged human mesenchymal stem cells: The duration of bone morphogenetic protein-2 stimulation determines induction or inhibition of osteogenic differentiation. Orthop Rev 2014;6:5242.

53 Baxter MA, Wynn RF, Jowitt SN et al. Study of telomere length reveals rapid aging of human marrow stromal cells following in vitro expansion. Stem Cells 2004;22:675–682.

54 Chen HT, Lee MJ, Chen CH et al. Proliferation and differentiation potential of human adipose-derived mesenchymal stem cells isolated from elderly patients with osteoporotic fractures. J Cell Mol Med 2012;16:582–593.

55 Ross SE, Hemati N, Longo KA et al. Inhibition of adipogenesis by Wnt signaling. Science 2000;289:950–953.

56 Ganguly P, El-Jawhari JJ, Giannoudis PV et al. Age-related changes in bone marrow mesenchymal stromal cells: A potential impact on osteoporosis and osteoarthritis development. Cell Transplant 2017;26:1520–1529.

57 Ishikawa H, Kitoh H, Sugiura F et al. The effect of recombinant human bone morphogenetic protein-2 on the osteogenic potential of rat mesenchymal stem cells after several passages. Acta Orthop 2007;78:285–292.

58 Bruderer M, Richards RG, Alini M et al. Role and regulation of RUNX2 in osteogenesis. Eur Cell Mater 2014;28:269–286.

59 Pountos I, Georgouli T, Henshaw K et al. The effect of bone morphogenetic protein-2, bone morphogenetic protein-7, parathyroid hormone, and platelet-derived growth factor on the proliferation and osteogenic differentiation of mesenchymal stem cells derived from osteoporotic bone. J Orthop Trauma 2010;24:552–556.

60 El Bialy I, Jiskoot W, Reza Nejadnik M. Formulation, delivery and stability of bone morphogenetic proteins for effective bone regeneration. Pharm Res 2017;34:1152–1170.

61 Fan J, Im CS, Guo M et al. Enhanced osteogenesis of adipose-derived stem cells by regulating bone morphogenetic protein signaling antagonists and agonists. Stem Cells Translational Medicine 2016;5:539–551.

62 Park KW, Waki H, Kim WK et al. The small molecule phenamil induces osteoblast differentiation and mineralization. Mol Cell Biol 2009;29:3905–3914.

See www.StemCellsTM.com for supporting information available online.